22 May 1998

ELSEVIER

Chemical Physics Letters 288 (1998) 487–493

CHEMICAL PHYSICS LETTERS

# Endoergic reactions of hyperthermal $C(^3P)$ with methane and acetylene

M.R. Scholefield, J.-H. Choi [1], S. Goyal [2], H. Reisler

*Department of Chemistry, University of Southern California, Los Angeles, CA 90089-0482, USA*

Received 2 December 1997; in final form 4 March 1998

**Abstract**

Endoergic reaction channels of $C(^3P)$ with $CH_4$ and $C_2H_2$ have been studied by using free laser ablation of graphite for preparation of hyperthermal ($> 2$ eV) $C(^3P)$. Energy distributions in the CH products are determined and compared with those obtained in other reactions of $C(^3P)$. It is suggested that both reactions proceed via carbene intermediates, but the specific mechanisms of the two reactions are different. © 1998 Elsevier Science B.V. All rights reserved.

## 1. Introduction

Atomic carbon is one of the smallest elements that participates in abstraction, addition and insertion reactions, which are important in combustion, interstellar and synthetic hydrocarbon chemistry [1–3]. Recently, we examined the reaction dynamics of hyperthermal ($\sim 2$ eV) atomic carbon ($^3P$) generated by laser ablation of graphite with $H_2$, HCl, HBr, and $CH_3OH$ by using crossed molecular beams, and probing the CH product via laser induced fluorescence (LIF) [4]. Based on theoretical investigations [5,6] and comparisons of the CH rotational distributions with those from the reactions of $C(^1D)$ with $H_2$ and HCl [7], it was suggested that the reactions of $C(^3P)$ proceed via an insertion mechanism involving the participation of carbene intermediates. This mechanism is also supported by trajectory calculations performed by Guadagnini and Shatz [8], which result in CH internal distributions in agreement with the experimental observations.

In this Letter, we describe our investigations of the endoergic H-atom transfer reactions of hyperthermal $C(^3P)$ with molecular beams of methane and acetylene [3]:

$$C(^3P) + CH_4 \rightarrow CH + CH_3\,, \quad \Delta H = +22.8 \pm 4.2 \text{ kcal/mol}\,, \qquad (1)$$

$$C(^3P) + C_2H_2 \rightarrow CH + C_2H\,, \quad \Delta H = +28.3 \pm 7 \text{ kcal/mol}\,. \qquad (2)$$

Reaction (1) is a prototype of a reaction of $C(^3P)$ with saturated hydrocarbons, while reaction (2) rep-

[1] Permanent address: Department of Chemistry, College of Science, Korea University, Anam-1-dong, Seongbuk-ku, Seoul, South Korea 136-701.

[2] Permanent address: Basawa Technologies, 5, Sarv Priya Vihar Market, New Delhi-110016, India.

[3] The energetics of the reactions are calculated for ground state reactants and products by using heats of formation taken from Ref. [9].

0009-2614/98/$19.00 © 1998 Elsevier Science B.V. All rights reserved.
PII: S0009-2614(98)00276-0

resents a case where an endoergic channel competes effectively with open exoergic channels [4,10–12]. As before [4], $C(^3P)$ is produced with the laser ablation source operating in the free ablation mode, since it generates $C(^3P)$ with translational energies $> 50$ kcal/mol. LIF is used to interrogate the CH diatomic product, yielding nascent rotational distributions, as well as spin-orbit and $\Lambda$-doublet propensities. The results are compared to our earlier studies of carbon atom reactions, and to recent experimental and theoretical work on the $C(^3P) + C_2H_2 \rightarrow C_3H + H$ system [10–12].

## 2. Experimental details

As the experimental apparatus has been described in detail elsewhere [4], only relevant features are presented here. The crossed beam apparatus consists of an ablation chamber, a molecular beam chamber and an octagonal reaction chamber, each pumped by a diffusion pump. Average pressures with both beams on are $\sim 4 \times 10^{-5}$ Torr.

Ground state atomic carbon, $C(^3P)$, is generated by free laser ablation of a spectroscopic grade graphite rod, maintained in constant helical motion. This produces a hyperthermal (0.5–10 eV), pulsed atomic beam of short temporal duration (6 $\mu$s fwhm). The rod is irradiated by 3–4 mJ pulses of the focused (50 cm focal length lens) 266 nm output of a Nd:YAG laser (Spectra-Physics GCR-11-3, 7 ns). The focal point is adjusted to maximize monomeric carbon concentrations and minimize carbon clusters by monitoring product CH signals and background $C_3$ fluorescence. Ablated carbon atoms are skimmed by a 3 mm skimmer and then expand freely into the reaction chamber. No metastable states of atomic carbon ($^1D$, $^1S$) have been observed in the laser ablation of graphite under our experimental conditions.

Pulsed, supersonic molecular beams of methane and acetylene are generated by expansion through a solenoid valve (General Valve, 0.8 mm diameter orifice, 750 $\mu$s fwhm) at stagnation pressures of $\sim 800$ Torr (300 K). The neutral beams are unskimmed, and neat gases are used in the expansion to obtain higher signal-to-noise ($S/N$) ratios. The pulsed valve is heated to $\sim 80$°C to minimize the formation of neutral beam clusters and is typically placed $\sim 30$ mm from the reaction center.

The $CH(X\,^2\Pi)$ product is probed by LIF via the $B\,^2\Sigma^- \leftarrow X\,^2\Pi$ transition using an excimer-pumped dye laser system (Questek 2220M and Lambda Physik FL2001) operating on QUI dye at $\sim 390$ nm. The probe beam is loosely focused to a $\sim 3$ mm spot at the reaction center by a 1 m focal length lens. The resulting fluorescence is imaged through a Galileo-type telescope onto the PMT (GaAs Hamamatsu R943-02) using appropriate filters. The probe laser pulse is typically delayed by 6 $\mu$s with respect to the firing of the ablation laser.

Analog signals from the PMT are sent to a Nicolet Explorer II digital oscilloscope interfaced to a computer for data storage and processing. The timing sequence of the experiments is controlled by an array of pulse and delay generators with 10 ns time resolution.

## 3. Experimental results and analysis

### 3.1. Center-of-mass collision energies

Velocity and kinetic energy distributions of $C(^3P)$ in the beam have been characterized in detail before using measurements of its time-of-flight [4]. The directional, monomeric carbon beam possesses a peak velocity of $\sim 8000$ m s$^{-1}$ with a broad velocity distribution of $\sim 6000$ m s$^{-1}$ fwhm. The estimated velocities of neat methane and acetylene are 1115 and 875 m s$^{-1}$, respectively, assuming full expansion [13]. The center of mass (CM) collision energies peak at 40 kcal/mol and extend to 130 kcal/mol for the $C + CH_4$ system, while the peak energy for the $C + C_2H_2$ reaction is at $\sim 48$ kcal/mol with a high energy tail extending to $\sim 160$ kcal/mol.

### 3.2. CH($X\,^2P$) internal state distributions

The $CH(X\,^2\Pi,\ v'' = 0)$ rotational distributions from reactions (1) and (2) have been determined from the LIF spectra of the $B\,^2\Sigma^- \leftarrow X\,^2\Pi$ transition [14–16]. Although highly endoergic, CH LIF signals with good $S/N$ were obtained for both reactions. Fig. 1 shows the CH spectrum from reaction (1), including the entire R-branch and portions of the Q- and P-branches. No vibrational excitation of the

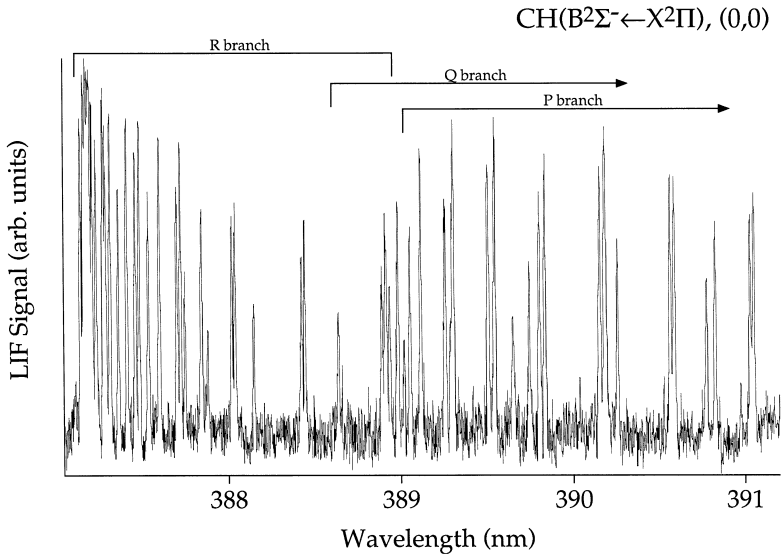


Fig. 1. CH $B\,^2\Sigma^- \leftarrow X\,^2\Pi$ ($v'' = 0$) LIF spectrum showing the entire R-branch and portions of the Q- and P-branches, obtained from the reaction of $C(^3P) + CH_4$.

CH product was observed in either reaction. Optimum $S/N$ ratios were obtained at an ablation-probe delay of 6 μs, corresponding to the peak of the $C(^3P)$ TOF distribution.

The spectra were assigned by comparisons with known line positions [14–16]. Relative rotational populations for the two spin-orbit states, $^2\Pi_{1/2}$ and $^2\Pi_{3/2}$, were derived from measured peak heights using established methods and assuming saturated conditions [4,7]. Fig. 2 displays the R- and Q-branch level populations for reactions (1) and (2). Also shown for comparison is the rotational distribution obtained for the $C + H_2$ reaction. As in previous cases, no spin-orbit preferences are observed, and therefore the displayed populations are the average for the two CH spin-orbit states. The distributions can be roughly assigned temperatures of $2200 \pm 100$ and $1800 \pm 200$ K for reactions (1) and (2), respectively. The corresponding average rotational energies (obtained from the weighted averages of the measured rotational populations) are 1100 and 920 $cm^{-1}$. Since the hyperthermal carbon beam leads to a broad distribution of collision energies, it is impossible to estimate the fractional partitioning of available energy into CH internal excitation.

$CH(X\,^2\Pi)$ Λ-doublet populations have been obtained for the reaction of $C(^3P)$ with methane. For a

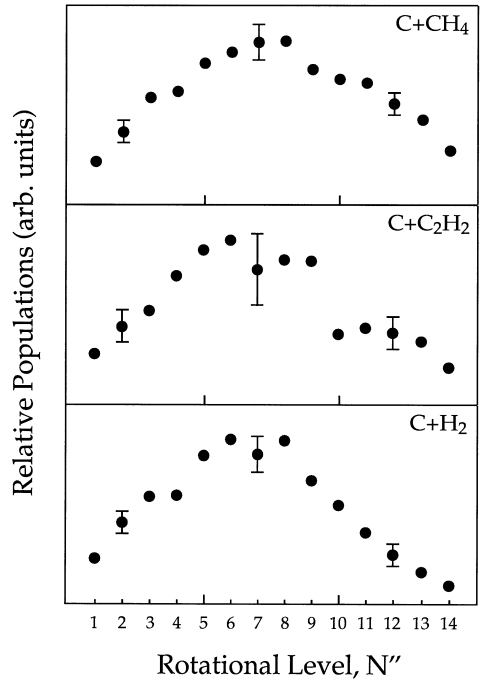


Fig. 2. $CH(^2\Pi,\ v = 0)$ rotational distributions obtained from the reactions of $C(^3P)$ with $CH_4$, $C_2H_2$ and $H_2$. Only the R-branch populations are displayed; however, similar distributions are obtained for the Q-branch populations. The data are obtained by averaging the CH $^2\Pi_{1/2}$ and $^2\Pi_{3/2}$ spin-orbit states, which are equally populated in all reactions.

$^2\Sigma \leftarrow {}^2\Pi$ transition, Q lines ($\Delta J = 0$) originate from $\Pi(A')$ $\Lambda$-doublet states, while P or R lines ($\Delta J = \pm 1$) originate from $\Pi(A'')$ states. Relative populations of the $\Lambda$-doublet components have been determined by a quantitative comparison of the rotational level populations of the Q- vs. R-branches shown in Fig. 1, assuming saturation and neglecting polarization and corrections for the degree of electron alignment [7,17,18]. No significant propensity for either $CH(X\,^2\Pi)$ $\Lambda$-doublet component is observed for $N'' = 3$–12. A slight increase in the $\Pi(A'')$ component at higher $N''$ is attributed to a decrease in the atomic carbon beam intensity in the course of the measurement.

## 4. Discussion

The observed rotational distributions of the $CH(X\,^2\Pi)$ product from reactions (1) and (2) are rather similar to those obtained in the endoergic reactions previously examined; i.e., $C(^3P)$ with $H_2$, HBr, HCl, and $CH_3OH$ [4] and $C(^1D)$ with $H_2$ [7]. Rotational temperatures ranging from 1500 to 2200 K were obtained, and no vibrational excitations were observed. In the case of $CH_4$, the $CH(X\,^2\Pi)$ $\Lambda$-doublet and spin-orbit components are equally populated within our experimental uncertainty, again in common with the endoergic reactions previously studied. Since the mechanisms governing the two title reactions are different, they are discussed separately below.

### 4.1. $C(^3P) + CH_4 \rightarrow CH + CH_3$

Although detailed calculations for this reaction are unavailable, recent high-level calculations performed by Harding, Guadagnini and Schatz (HGS) on the reaction $C(^3P) + H_2 \rightarrow CH + H$ provide valuable insights [6]. HGS obtained a global ground-state potential energy surface (PES) for all orientations of atomic carbon approach, and found that direct H-atom abstraction via a collinear $C_{\infty v}$ path along the $^3\Pi$ surface has a high barrier, while instead, a reaction via the insertion mechanism can proceed without a barrier and therefore predominates. The barrier is lowered as a result of a conical intersection between the $^3A_2$ and $^3B_1$ states in the perpendicular $C_{2v}$ approach (or between the corresponding $A''$ states in the off-perpendicular $C_s$ approach). The excited $^3A_2$ state derives from an approach of $C(^3P)$ in which the empty p orbital points towards $H_2$, while the $^3B_1$ state is the ground state of the methylene intermediate. In more recent reactive trajectory simulations [8], Guadagnini and Schatz obtained product internal distributions and $\Lambda$-doublet propensities that are in excellent agreement with the experimental measurements obtained in our crossed beam study of the $C(^3P) + H_2$ reaction [4].

Based on the available experimental and theoretical results, we suggest that the $C(^3P) + CH_4$ reaction proceeds through a similar insertion pathway involving the $HCCH_3$ carbene intermediate: (1) in the exoergic reaction of $C(^3P)$ with $CHCl_3$ carried out at low, well-defined collision energies the CCl product exhibits a statistical energy disposal (prior model), supporting a reaction mechanism proceeding via a long-lived intermediate [19]; (2) the similarity in the spin-orbit, rotational, and $\Lambda$-doublet distributions in all the reactions studied so far is suggestive of a common underlying mechanism; and (3) the importance of an empty orbital of the reactant in directing reactivity at long range has been recognized in other insertion reactions, e.g., those of carbenes with hydrocarbons [1,20]. An approach in which the reactant's empty orbital points towards a closed-shell molecule promotes attractive interactions at long range and may precede the insertion step. Indeed, in the theoretical work on the $C(^3P) + H_2$ reaction, such an approach proved crucial to lowering the insertion barrier. Thus, the combined evidence strongly argues in favor of an insertion mechanism promoted by attractive long range interactions between the empty p orbital on carbon and the closed-shell $CH_4$, and proceeding via a triplet $^3HCCH_3$ intermediate.

The heat of formation of $^3HCCH_3$ was obtained in theoretical work on the $C(^3P) + CH_4 \rightarrow {}^3HCCH_3$ insertion reaction [21], where the optimized geometry of $^3HCCH_3$ and the insertion pathway on the electronic ground state PES were examined. It was found that $^3HCCH_3$ is 61.5 kcal/mol more stable than the reactants, but a barrier to insertion of 30.6 kcal/mol existed in the entrance channel. However, unlike the HGS calculations, the participation of excited electronic states deriving from different ori-

entations of the atomic carbon 2p orbitals with respect to methane was not considered, nor was the possibility of lowering the insertion barrier due to surface crossings. Nevertheless, it is possible to gain insight regarding the mechanism using the HGS results for the $C(^3P) + H_2$ system [6]. According to Sakai et al. [21], the $^3HCCH_3$ intermediate is of $C_s$ symmetry, and this symmetry is conserved throughout the reaction. Thus, assuming $C_s$ symmetry for the other electronic states of the intermediate, there will be three degenerate triplet states, one $^3A''$ and two $^3A'$. At large separations the $^3A''$ state for which the empty 2p orbital of the carbon atom is oriented towards a C–H bond will be the lowest in energy due to smaller repulsions. An avoided crossing between the two $^3A'$ states at shorter distances can lower the insertion barrier significantly, in analogy with the $C(^3P) + H_2$ reaction. If the symmetry is further reduced during the reaction, the avoided crossings among the triplet electronic states will become even more likely. We note that the CH signals from the reaction of $C(^3P) + CH_4$ are only slightly lower than those from $C(^3P) + H_2$, indicating that the barrier to insertion is not substantial.

The existence of a low-lying singlet $^1HCCH_3$ state, calculated to be $\leq 5.2$ kcal/mol above the ground triplet state [22,23], may contribute to strong mixings leading to the observed absence of Λ-doublet preferences. Singlet–triplet surface crossings are common in carbenes [24], and $^1HCCH_3$ is nonplanar according to calculations [21], which should also lead to reduced Λ-doublet preferences in the CH product. Thus, all the evidence is consistent with an insertion mechanism.

In the reaction of $C(^3P)$ with methane and other saturated hydrocarbons, the spin-orbit states of CH are equally populated [4]. It is instructive to compare these results to the corresponding reactions of $O(^3P)$, which are thought to proceed via collinear abstraction and exhibit significant preferences for populating the lowest spin-orbit state of $OH(^2\Pi)$ [25–29]. In discussing spin-orbit propensities in the $O(^3P) + CH_4$ reaction, McKendrick and co-workers suggest that $\Omega$, the projection of the electronic angular momentum on the internuclear axis, is conserved during the reaction, while strong long-range entrance and exit channel interactions lead to efficient mixings among spin-orbit states with the same $\Omega$ value [28,29]. These interactions result in a propensity towards populating the lowest spin-orbit state of the OH product, as observed experimentally. For the $C(^3P) + CH_4$ reaction proceeding via insertion through a strongly coupled collision complex, there is no reason to expect $\Omega$ to be conserved in the course of the collision. Also, the existence of several low-lying electronic states of the intermediate will further enhance nonadiabatic transitions, since several attractive electronic states can correlate to each spin-orbit state of the CH product. Thus, adiabaticity is not expected to persist, and the equal populations of the CH spin-orbit states are in accordance with the proposed insertion mechanism.

### 4.2. $C(^3P) + C_2H_2 \rightarrow CH + C_2H$

The most surprising result concerning reaction (2) is the fact that significant CH signals are obtained from this highly endoergic channel despite the presence of several exoergic channels leading to $C_3H$ + H. This stands in contrast to the reaction of $C(^3P)$ with chloroform, in which the endoergic CH channel ($\Delta H = +14.4$ kcal/mol) was barely discernible in competition with the exoergic CCl channel [19]. According to Kaiser et al. [10], the exoergic channels for the $C(^3P) + C_2H_2$ reaction at low ($\leq 10.8$ kcal/mol) collision energies yield $C_3H$ products in either the linear and/or the cyclic forms, *l*-$C_3H$ and *c*-$C_3H$. The overall reaction is very fast, with a room temperature rate coefficient of $(2.0 \pm 0.1) \times 10^{-10}$ $cm^3$ $molecule^{-1}$ $s^{-1}$ [30].

Detailed ab initio calculations show that the $^3C_3H_2$ triplet diradical intermediate formed by the interaction of $C(^3P)$ with the π electron density of acetylene can have four stable structural isomers [12]. From the combined experimental and theoretical work, it is concluded that the observed $C_3H$ signal derives predominantly from two microchannels. The first microchannel involves initial formation of *s*-trans propenediylidene, HC(C)CH

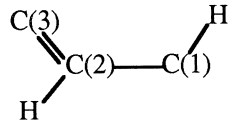


. HC(C)CH undergoes a [2,3] H-shift (where C(3) is the terminal carbon, and C(2) is adjacent to it) to

yield propargylene (HCCCH) — the lowest energy, symmetric isomer, which dissociates to yield *l*-$C_3H$. Another microchannel giving rise to forward scattered cyclic *c*-$C_3H$ is attributed to direct dissociation of a second reaction intermediate, cyclopropenylidene (*c*-$C_3H_2$). However, experimental evidence indicates that the cross-section for formation of *c*-$C_3H_2$ diminishes rapidly as the collision energy increases [10–12].

The HC(C)CH intermediate arises from the interaction between two p electrons of $C(^3P)$ and two acetylenic $\pi$ molecular orbitals to form a pair of $\sigma$ and $\pi$ bonds between C(3) and C(2) [12]. This approach geometry leads to maximum orbital overlap, and therefore initial formation of the HC(C)CH intermediate is probably the favored entrance channel. At low collision energies (e.g., $\leq 10$ kcal/mol), the lifetime of the HC(C)CH intermediate is sufficiently long to allow the [2,3] H-shift needed to generate the HCCCH isomer, which then decomposes to *l*-$C_3H + H$ as observed.

At the much higher collision energies employed in our experiments, we estimate that the lifetime of the HC(C)CH intermediate (which is bound by only $\sim 32$ kcal/mol with respect to the reactants [11]) will become too short to allow an efficient [2,3] H-shift to occur, and other open channels will start to compete. For example, HC(C)CH may directly decompose to $CH + C_2H$, a channel which is now energetically allowed. If bond cleavage involves the C(2)–C(1) bond, no isomerization is necessary, and this simple bond fission reaction, which possibly proceeds without a barrier, can compete favorably with the isomerization step with its associated tight transition state. We note that at their equilibrium positions, the C(3)–C(2) and C(2)–C(1) bond lengths are comparable (1.349 and 1.392 Å, respectively) [10–12], and fission of the C(2)–C(1) bond is likely. Therefore, once the $CH + C_2H$ channel opens, its yield relative to the H-shift channel should rise rapidly with collision energy. We note that an abstraction reaction yielding CH is also a possibility at these high collision energies.

## 5. Summary

The two title endoergic reactions of $C(^3P)$ have been examined at high collision energies by using LIF detection of the CH product. Based on the CH product state distributions and comparisons with other experimental and theoretical results, it appears that both these reactions, which involve saturated and unsaturated hydrocarbons, evolve via carbene intermediates. In the case of reaction (1), we suggest that the barrier to insertion of $C(^3P)$ into a C–H bond is lowered by surface crossings in the entrance channel, in analogy with the $C(^3P) + H_2$ reaction. In the case of reaction (2), it is possible that the endoergic pathway yielding CH evolves via direct dissociation of the initially formed HC(C)CH addition intermediate. This pathway, once open, will compete effectively with the exoergic channel yielding *l*-$C_3H + H$, which requires an additional, relatively slow, isomerization step to the HCCCH intermdiate.

## Acknowledgements

This study was supported by the director, Office of Energy Research, Office of Basic Sciences, Chemical Sciences Division of the US Department of Energy, under Grant DEFG03-88ER13959.

## References

[1] C. Mackay, in: R.A. Moss, M. Jones (Eds.), Carbenes, vol. II, Wiley, New York, 1975.
[2] P.B. Shevlin, in: R.A. Abramovich (Ed.), Reactive Intermediates, vol. I, Plenum, New York, 1980.
[3] R.D. Levine, R.B. Bernstein, Molecular Reaction Dynamics and Chemical Reactivity, Oxford University Press, New York, 1987.
[4] M.R. Scholefield, S. Goyal, J.-H. Choi, H. Reisler, J. Phys. Chem. 99 (1995) 14605.
[5] L.B. Harding, J. Phys. Chem. 87 (1983) 441.
[6] L.B. Harding, R. Guadagnini, G.C. Schatz, J. Phys. Chem. 97 (1993) 5472.
[7] D.C. Scott, J. de Juan, D.C. Robie, D. Schwartz-Lavi, H. Reisler, J. Phys. Chem. 96 (1992) 2509.
[8] R. Guadagnini, G.C. Schatz, J. Phys. Chem. 100 (1996) 18944.
[9] M.W. Chase Jr., C.A. Davies, J.R. Downey Jr., D.J. Frurip, R.A. McDonald, A.N. Syverud, J. Phys. Chem. Ref. Data 14 (1985), Suppl. 1 JANAF Thermochemical Tables, 3rd ed., Part I.
[10] R.I. Kaiser, C. Ochsenfeld, M. Head-Gordon, Y.T. Lee, A.G. Suits, J. Chem. Phys. 106 (1997) 1729.
[11] R.I. Kaiser, C. Ochsenfeld, M. Head-Gordon, Y.T. Lee, A.G. Suits, Science 274 (1996) 1508.

[12] C. Ochsenfeld, R.I. Kaiser, Y.T. Lee, A.G. Suits, M. Head-Gordon, J. Chem. Phys. 106 (1997) 4141.
[13] E. Kolodney, A. Amirav, Chem. Phys. 82 (1983) 269.
[14] C.E. Moore, H.P. Broida, J. Res. Natl. Bur. Stand. 63A (1959) 19.
[15] L. Gerö, Z. Phys. 118 (1941) 27.
[16] G. Herzberg, J.W.C. Johns, Astrophys. J. 158 (1969) 397.
[17] P. Andresen, E.W. Rothe, J. Chem. Phys. 82 (1985) 3634.
[18] M.H. Alexander et al., J. Chem. Phys. 89 (1988) 1749 (and references therein).
[19] J.-H. Choi, M.R. Scholefield, D. Kolosov, H. Reisler, J. Phys. Chem. 101 (1997) 5846.
[20] R.D. Bach, M.-D. Su, E. Aldabbagh, J.L. Andres, H.B. Schlegel, J. Am. Chem. Soc. 115 (1993) 10237.
[21] S. Sakai, J. Deisz, M.S. Gordon, J. Phys. Chem. 93 (1989) 1888.
[22] M.M. Gallo, H.F. Schaefer III, J. Phys. Chem. 96 (1992) 1515.
[23] T.-K. Ha, M.T. Nguyen, L.G. Vanquickenborne, Chem. Phys. Lett. 92 (1982) 459.
[24] H. Petek, D.J. Nesbitt, C.B. Moore, F.W. Birss, D.A. Ramsay, J. Chem. Phys. 86 (1987) 1189.
[25] P. Andresen, A.C. Luntz, J. Chem. Phys. 72 (1980) 5842.
[26] A.C. Luntz, J. Chem. Phys. 73 (1980) 1172.
[27] K. Kleinemanns, A.C. Luntz, J. Chem. Phys. 77 (1982) 3537.
[28] G.M. Sweeney, A. Watson, K.G. McKendrick, J. Chem. Phys. 106 (1997) 9172.
[29] G.M. Sweeney, A. Watson, K.G. McKendrick, J. Chem. Phys. 106 (1997) 9182.
[30] H. Nazre, D. Husain, J. Photochem. Photobiol. A: Chem. 70 (1993) 119.